Structural Basis of Fluorescence Fluctuation Dynamics of Green Fluorescent Proteins in Acidic Environments

Yuexin Liu, Hye-Ryong Kim, and Ahmed A. Heikal*

Department of Bioengineering, The Pennsylvania State University, 231 Hallowell Building, University Park, Pennsylvania 16802

Received: April 6, 2006; In Final Form: September 6, 2006

Green fluorescent proteins (GFPs) have become powerful markers for numerous biological studies due to their robust fluorescence properties, site-specific labeling, pH sensitivity, and mutations for multiple-site labeling. Fluorescence correlation spectroscopy (FCS) studies have indicated that fluorescence blinking of anionic GFP mutants takes place on a time scale of 45−300 ms, depending on pH, and have been attributed to external proton transfer. Here we present experimental evidence indicating that conformational change in the protein β-barrel is a determining step for the external protonation of GFP−S65T (at low pH) using time-resolved fluorescence and polarization anisotropy measurements. While the average anionic fluorescence lifetime of GFP−S65T is reduced by ∼18% over a pH range of 3.6−10.0, the fluorescence polarization anisotropy decays mostly as a single exponential with a rotational time of $\phi = 17 \pm 1$ ns, which indicates an intact β-barrel with a hydrodynamic volume of 78 ± 5 nm^3. In contrast, the total fluorescence (525 ± 50 nm) of the excited neutral state of S65T reveals a strong correlation between the fluorescence lifetime, structural conformation, and pH. The average fluorescence lifetime of the excited neutral state of S65T as a function of pH yields p$K_a \approx 5.9$ in agreement with literature values using steady-state techniques. In contrast to the intact β-barrel at high pH, the anisotropy of neutral S65T (at pH ≤ pK_a) decays as a biexponential (e.g., at pH 5.8, $\phi_1 = 1.86$ ns, $\beta_1 = 0.03$, $\phi_2 = 17.5$ ns, and $\beta_2 = 0.25$), which suggests a segmental mobility of the chromophore associated with conformational changes of the protein. The segmental motion of the S65T chromophore becomes faster with an enhanced amplitude ratio as pH is reduced. For comparative purposes, we also provide complementary FCS results on fluorescence blinking of the excited neutral state of an EGFP mutant (F64L/S65T) on a much slower time scale. Our results indicate that conformational rearrangement of the β-barrel and the amino acids surrounding the embedded chromophore is a rate-determining step for external proton transfer and possibly cis/trans isomerization as nonradiative pathways that underlie fluorescence blinking of GFP mutants in an acidic environment. In addition, the neutral-state transition is likely to be involved in the blinking process previously observed for the anionic-state transition in several GFP mutants.

1. Introduction

Green fluorescent proteins (GFPs), from the jellyfish *Aequorea victoria*, have been widely used as fluorescence markers in a wide range of cell studies.[1,2] The GFP chromophore is formed by an intermolecular autocatalytic reaction between amino acids Ser65, Tyr66, and Gly67.[3,4] The β-barrel shields the chromophore from external quenchers[5,6] and provides steric hindrance that prevents the cis/trans isomerization pathway,[7,8] which explains the superb fluorescence properties of GFP mutants, even when fused with other proteins.[5,6] Recent theoretical calculations on a GFP-like chromoprotein (asFP595, isolated from *Anemonia sulcata*) have suggested that the nonfluorescent (dark) state is associated with a trans configuration of the embedded chromophore.[7,8] In contrast, molecular dynamics calculations of the GFP chromophore indicate that the trans and cis conformations of the GFP chromophore exhibit indistinguishable energy minima.[44] As a result, GFP mutants provide interesting model systems for studying the underlying mechanisms of their unique photophysical properties, which can be exploited for quantitative biological studies.

There have been recent efforts to develop new GFP variants with minimized sensitivity to pH, chloride ion concentration [Cl^-], and photobleaching.[9,10] Yellow fluorescent protein (YFP) mutant, T203Y, has remarkable pH resistance and may find use in the labeling of acidic organelles.[9] Citrine, from the third generation of YFP derivatives, exhibits a reduced sensitivity to [Cl^-], a larger pK_a value suited to physiological pH, and improved fluorescence properties.[11] There is a strong demand for red fluorescent proteins for (i) multiccolor protein-tracking applications, (ii) new donor−acceptor pairs for fluorescence resonance energy transfer (FRET) studies of molecule−molecule interactions, and (iii) distinctive emission from the underlying cellular autofluorescence.[12] Applications of DsRed (a red fluorescent protein isolated from a coral of the *Discosoma* genus)[12,13] to cell and protein studies are limited due to its tetramerization[14,15] and long maturation time.[9] Tsien and coworkers engineered a monomeric DsRed variant (mRFP1) that matures quickly.[9,10] Recently, a new generation of intrinsically red fluorescent protein (RFP) mutants (e.g., mRFP1, mCherry, mOrange, and mStrawberry) has been reported[16] with superb spectroscopic properties such as large extinction coefficients, high fluorescence quantum yields, and long absorption and emission wavelengths. An alternative approach has been

* Author to whom correspondence should be addressed. Phone: (814) 865-8093. Fax: (814) 865-0496. E-mail: aah12@psu.edu.

10.1021/jp062164t CCC: $33.50
Published on Web 11/03/2006

proposed to generate long-wavelength fluorescence emission using a photoactivation mechanism.[17] Stepanenko et al. have provided a systematic comparison between green and red fluorescent proteins, concerning their structural properties and conformational stabilities, using steady-state, Stern−Volmer quenching and circular dichroism (CD) spectroscopy.[18]

GFP mutants exhibit both neutral- and anionic-state conformers[2,3,6] with electronic transitions at 396 and 488 nm (or longer), respectively, whereas the fluorescence quantum yield of the latter is much higher[19,20] than the former. As a result, numerous GFP mutations have been created to enhance the anionic-state population with variable emission peaks (from blue to yellow) for multiple-site labeling and FRET studies. Dickson and coworkers reported fluorescence blinking of T203Y and T203F mutants upon 488 nm (anionic) excitation and a subsequent recovery following 405 nm (neutral) illumination.[21] Despite the two different absorption bands, GFP emits mainly around 505 nm due to the excited-state deprotonation of the hydroxyl group of Tyr66.[22,23] A minor emission shoulder around 457 nm of EGFP was assigned to the neutral-state emission.[3,24] The population of the neutral state of GFP increases as the proton concentration increases in the surrounding bulk solution. Such interconversion between the anionic (bright) and neutral (relatively dark) states of GFP was assigned as the underlying mechanism for fluorescence blinking observed in fluorescence correlation spectroscopy (FCS) studies.[15,25,26] Anionic GFP mutants (e.g., GFP−S65T, EGFP, citrine, T203Y, and T203F) exhibit fluorescence blinking that takes place on a time scale of ∼45−340 μs due to external proton transfer from the buffer solution to the protein interior.[15,25,26] However, it remains unclear whether structural changes in the β-barrel of GFP are necessary for such proton exchange between low-pH buffer and the protein interior. Furthermore, it is not yet clear whether the underlying mechanisms for GFP blinking in FCS studies are the same as those observed in single-molecule studies, which reveal a slow (seconds) blinking process.[21,27]

Enoki et al. have investigated the acid denaturation and folding/unfolding kinetics of a GFP mutant (cycle 3, F99S/M153T/V163A) by measuring the chromophore and tryptophan fluorescence.[28] Using far-UV CD with a stopped-flow system, they have demonstrated that the refolding kinetics of the acid-denatured (at pH 1.5 and 2.0) state of cycle 3 involve five kinetic phases.[28] In addition, the slow phase was fully rate-limited by slow isomerization in the denatured and intermediate states. Molecular dynamics (MD) simulations of GFP have also been carried out to investigate the conformational rearrangements induced by deprotonation.[29] In addition to MD studies, the authors also used quantum mechanics/molecular mechanics (QM/MM) to investigate the β-barrel effects on the internal rotation of the chromophore, while providing a quantitative estimate of the torsional rotation barrier around the bridging bond.[29] Real-time experimental measurements of acid-induced, ultrafast conformational changes of GFP remain elusive.

Here, we use time-resolved fluorescence lifetime and polarization anisotropy to address the correlation between the ultrafast conformational changes of a GFP−S65T mutant (as a model system) and the loss of its fluorescence (i.e., blinking) in acidic environments. We also investigate the neutral-state blinking kinetics of EGFP using FCS under 396 nm excitation. These results will be discussed in terms of a three electronic state transition model[30] to explain the blinking pathways in GFP and the excited-state dynamics of neutral and anionic GFP−S65T.

2. Materials and Methods

GFP−S65T mutant (S65T hereafter) was a generous gift from the group of Professor Stephen Benkovic (Department of Chemistry, Penn State University). The stock solution of the protein (30 mM) was then diluted in buffer solutions of varying pH (pH 3.6−10). Potassium phosphate (0.1 mM) buffers (for pH 6−8 range) were prepared from potassium monobasic and dibasic solutions. Solutions of 0.1 mM glacial acetic acid and sodium borate were used to prepare pH 3.0−5.5 and pH 8.5−10 buffer solutions, respectively. The desired pH was adjusted with a small amount of NaOH (0.5 mM). Absorption spectra were measured with a single-beam, diode array spectrophotometer (DU800, Beckman Coulter), whereas the fluorescence spectra were recorded using a PTI-QM-1 spectrofluorimeter (FL3-21, Fluorolog). The second harmonic (SHG4500, Coherent) of Ti:sapphire femtosecond laser pulses (∼120 fs at 76 MHz, Mira900F, Coherent) was used for 1P excitation of both the neutral- (396 nm) and the anionic- (488 nm) state transitions of S65T. The pulse repetition rate was reduced to 4.22 MHz using a pulse picker (Mira900, Coherent) before steering the laser pulses to the sample via the back entrance port of an inverted microscope (IX81, Olympus) and a dichroic mirror (488LP, Chroma). The filtered (using 525 ± 50, 525 ± 25, or 475 ± 25 nm filters from Chroma) epifluorescence was split into two channels using a 50/50 beam splitter, and the detection polarization of each was selected independently using Glan-Thompson polarizers for time- and polarization-resolved fluorescence measurements. The polarized fluorescence was detected by microchannel plate (MCP) (R3809U-50, Hamamatsu), amplified, and then fed to a time-correlated single-photon counting module (SPC-830, Becker and Hickl, Germany). The back aperture of a 1.2 NA objective (60×, water immersion, Olympus) was underfilled to minimize depolarization effects.[31]

2.1. Time-Resolved Fluorescence and Polarization Anisotropy. A nonlinear least-squares fitting routine (SPCM, Becker & Hickl, Germany) was used to analyze the measured magic angle (54.7°) fluorescence decays, $F(t)$, that are convoluted with the system response function, $R(t)$, (full width at half-maximum (fwhm), 50 ± 5 ps). Generally, the deconvoluted fluorescence decay is best described as a sum of exponentials with time constants (τ_i) and amplitudes (α_i) that are dependent on pH and electronic state transitions (i.e., anionic versus neutral)[3]

$$I_{54.7}(t) = R(t) \otimes F(t) = \sum_{i=1}^{3} \alpha_i \exp(-t/\tau_i) \qquad (1)$$

The average fluorescence lifetime is calculated as $\langle \tau_{fl} \rangle = \sum_i \alpha_i \tau_i / \sum_i \alpha_i$. The excited-state fluorescence decay rate ($k_{fl} = 1/\tau_{fl}$) of a given fluorophore is dependent on the radiative (k_r) and nonradiative (k_{nr}) rates as follows:[32] $k_{fl} = k_r + k_{nr}$. While the radiative rate is inherent in the molecular structure of the chromophore, the nonradiative processes may include isomerization, charge transfer, and ionization pathways that compete with fluorescence. As a result, the reduction of excited-state lifetime of a fluorophore can be attributed to the enhanced nonradiative processes under certain conditions. However, the identification of the underlying nonradiative processes is not straightforward and requires systematic studies of the excited-state dynamics in different environments and with targeted structural manipulations.

For time-resolved fluorescence polarization anisotropy, the measured parallel ($I_{||}(t)$) and perpendicular ($I_{\perp}(t)$) fluorescence decays were used to calculate the anisotropy decay as follows[32]

$$r(t) = [I_{\parallel}(t) - G \cdot I_{\perp}(t)]/[I_{\parallel}(t) + 2G \cdot I_{\perp}(t)] \quad (2)$$

The *G*-factor, which accounts for the polarization sensitivity of the detection channels, was estimated using a tail matching[32] approach for fluorescein emission under the same excitation and detection conditions. On the basis of the complexity of the molecular system, the anisotropy decays were either described as a single exponential (e.g., GFP in high pH buffer) or a complex multiexponential (e.g., GFP in low-pH buffer), which can be generally described as[32]

$$r(t) = \sum_{i=1}^{3} \beta_i \exp(-t/\varphi_i) \quad (3)$$

where the sum of the preexponential factors (β_i) equals the initial anisotropy (r_0). When the fluorophore undergoes a segmental motion while tethered with a large biomolecule, the corresponding rotational time (φ_i) becomes too slow to observe within the excited-state lifetime. As a result, the corresponding preexponential factor becomes assigned as a residual anisotropy (r_∞). The rotational time (φ) is related to the hydrodynamic volume (V) of a chromophore by the following relationship:[32] $\varphi = \eta V/K_B T$, where η is the viscosity of the buffer ($\sim$0.89 cP) at a given temperature ($T \approx 293$ K), and K_B is the Boltzmann constant.

2.2. Fluorescence Correlation Spectroscopy. The autocorrelation function of rhodamine green (lateral diffusion coefficient $D_{RhG} \approx 2.8 \times 10^{-6}$ cm^2/s)[15] was measured to calibrate the FCS setup that includes femtosecond laser pulses (at 82 MHz), an underfilled 1.2 NA, 60×, water-immersion objective, and a fiber (50 μm in diameter) that serves as a confocal pinhole. The autocorrelation function $G(t)$ is defined as[15,25,26] $G_D(\tau) = [\delta F(t)\delta F(t+\tau)]/\langle F(t)\rangle^2$, where $F(t)$ is the fluorescence intensity at a given time t and $\delta F(t)$ is the corresponding fluorescence fluctuation. The autocorrelation function of rhodamine green is best described by diffusion such that[15,25,26]

$$G_D(\tau) = \frac{1}{N}\frac{1}{(1+\tau/\tau_D)}\left[\frac{1}{(1+\tau/\omega^2\tau_D)}\right]^{0.5} \quad (4)$$

where N is the average number of molecules with a residence diffusion time of τ_D (for RhG, $\tau_D = 440 \pm 10$ ms) in the open three-dimensional Gaussian observation volume with an axial-to-lateral dimension, ω ($\sim$5.5 for this setup). In addition to diffusion, however, it is known that GFP exhibits fluorescence blinking processes (i.e., light- and pH-dependent), both of which are much faster than the overall diffusion of GFP molecules. The autocorrelation function due to these two blinking processes can be expressed as[15,25,26]

$$G_B(\tau) = [1 - f_{B1} + f_{B1}\exp(-\tau/\tau_{B1})][1 - f_{B2} + f_{B2}\exp(-\tau/\tau_{B2})] \quad (5)$$

where f_{Bi} is the amplitude fraction of the GFP population that undergoes blinking ($i = 1$ or 2 for light- or pH-driven processes, respectively)[25] over a time constant τ_{Bi}. Such a relationship is only valid when the time scales of these blinking processes are significantly different, which might not be the case at a very low pH or high excitation intensities.

3. Results and Discussion

3.1. Steady-State Spectroscopy of the Anionic and Neutral-State Transitions in S65T. The absorption, emission, and excitation spectra of S65T were measured at pH 10 and 5 (Figure 1). The observed general trend here is similar to those of other literature studies,[3,25] where the absorption band of anionic S65T at 488 nm ($\epsilon_{488} \approx 56\,000$ M^{-1} cm^{-1})[1,2] is reduced as pH decreases, with a concomitant increase in the neutral-state absorption at $\sim$392 nm and an isobestic point at $\sim$445 nm (Figure 1A).[25] In addition to the main emission band at $\sim$509 nm (pH 10), a new blue emission shoulder appears around 450 nm as the pH decreases (Figure 1B). To assign the transition associated with the observed blue emission shoulder at 450 ± 25 nm, we have measured the excitation spectra of S65T as a function of pH (5 and 10) and detection wavelength (450 nm) as shown in Figure 1C. At pH 10.0, the absorption and excitation spectra are basically congruent when the emitted fluorescence was detected at 510 nm. However, an excitation shoulder can be identified around 396 nm at pH 5.0, even with 510 nm detection (data not shown). Interestingly, when the fluorescence was detected at 450 nm, the excitation band at 396 nm was identical to the neutral absorption at low pH (Figure 1C). These results enable us to assign the blue emission shoulder around 450 nm (Figure 1B) to the excited neutral-state emission with

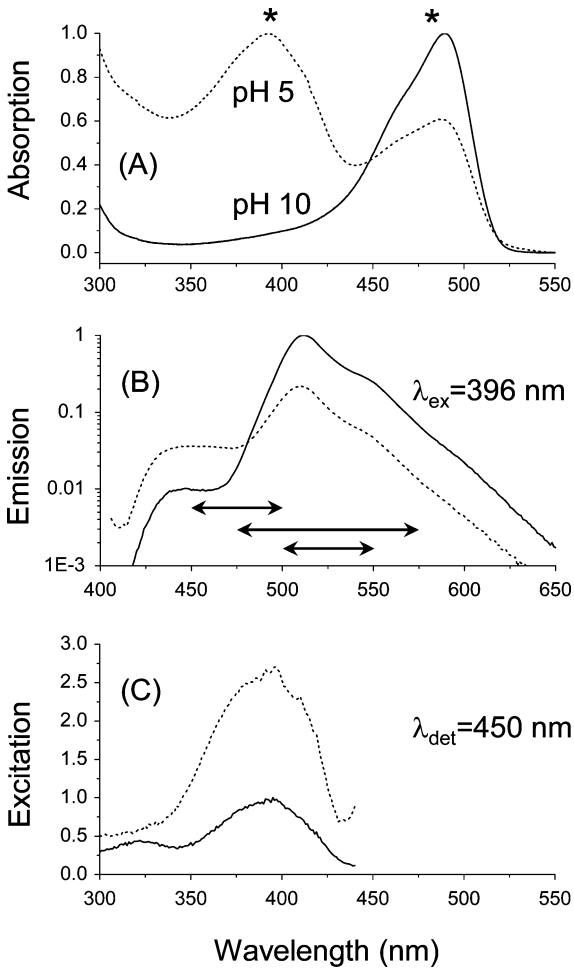

Figure 1. Steady-state spectroscopy of GFP−S65T sensitivity to the environmental pH. (A) In addition to the main absorption band of S65T (pH 10.0, solid line), a new absorption band appears around 392 nm (pH 5.0), which is assigned to the neutral-state transition (dotted line). The asterisks correspond to the excitation wavelengths used in this work. (B) The anionic-state emission of S65T peaks around 509 nm (pH 10) and is reduced significantly at a lower pH (5.0). Depending on the excitation wavelengths (480 or 396 nm), the detection filter bandwidths used here were varied as represented by the horizontal arrows (525 ± 25, 525 ± 50, and 475 ± 25 nm) shown above for guidance. In addition, an enhanced emission shoulder around 450 nm can be identified at pH 5.0, which is assigned to the neutral state transition as shown in the excitation spectrum (C) under 396 nm excitation.

TABLE 1: pH Dependence of the Time-Resolved Fluorescence of Anionic S65T When Excited at 480 nm[a]

pH	τ_1 (ps)	α_1	τ_2 (ns)	α_2	τ_3 (ns)	α_3	$\langle\tau_{fl}\rangle$ (ns)
8.0					2.95(1)[b]	1.0	2.95(1)
5.0			2.4(1)	0.46(8)	3.04(2)	0.54(8)	2.75(1)
4.5			2.32(2)	0.50(4)	3.03(7)	0.51(4)	2.68(3)
4.0			2.16(3)	0.35(2)	3.05(6)	0.47(1)	2.58(2)
3.6	87(11)	0.38(2)	1.29(6)	0.34(2)	3.82(2)	0.28(1)	1.54(6)

[a] The fluorescence is detected at 525 ± 25 nm using magic angle (54.7°) polarization with 24.4 ps/channel. [b] The number in parentheses represents the standard deviation (uncertainty) of the last digit.

a low quantum yield based on the time-resolved fluorescence measurements (see below).[3,4] Furthermore, a small portion of the neutral-state emission of S65T (excited at 396 nm) can be detected around 510 nm. Such spectral overlap between the neutral and anionic transitions might also explain the observed pH-dependent blinking in FCS studies[15,25,26] under 488 nm excitation. The absorption and emission bands associated with anionic S65T disappear at pH 4, while the neutral-state transition of the denatured protein dominates with absorption at 382 nm (with a roughly estimated extinction coefficient of $\epsilon_{382} \approx 44\,600$ M^{-1} cm^{-1}) and emission shoulder around ~450 nm (data not shown). The reduced extinction coefficient of the neutral-state transition of S65T at pH 4 is in agreement with that of Haupts et al.,[25] but it is not yet clear if such reduction can explain the loss of the neutral emission as was previously proposed (see below).[25]

It has been shown that fluorescence emission of anionic GFP mutants (e.g., S65T, EGFP, citrine, or pHfluorin)[15,25,26] is very sensitive to pH due to external proton transfer from low-pH buffer to the protein interior in a single-protonation step,[33,34] with a standard free reaction energy $\Delta G° = 33 \pm 1$ kJ/mol for S65T at room temperature.[25] Such pH sensitivity of GFP fluorescence has been exploited in various biological applications.[35,36] It is not clear, however, whether the external protonation that underlies the fluorescence blinking of GFP mutants[15,25,26] at low pH is correlated with conformational changes of the β-barrel. To address this question, we conducted time-resolved fluorescence lifetime and polarization anisotropy measurements on S65T, as a function of pH and excitation wavelengths. Furthermore, we used the absorption and emission spectra for qualitative analysis of the radiative rate constant of both anionic and neutral-state transitions (see below) using the Strickler−Berg equation.[32]

3.2. Excited Anionic-State Dynamics of S65T Less Sensitive to pH. *3.2.1. pH Effects on the Excited Anionic-State Lifetime of S65T.* At high pH, the excited ($\lambda_{ex} = 480$ nm) anionic-state fluorescence (525 ± 25 nm) decay of S65T can be described satisfactorily as a single exponential with a time constant of 2.95 ± 0.01 ns (Table 1, Figure 2D). These results are consistent with previous studies using the single-photon counting technique.[3,4] Assuming a fluorescence quantum yield of 0.66[1], the estimated radiative rate constant (k_r) is ~2.20×10^8 s^{-1}, using the measured fluorescence decay rate ($k_{fl} = 1/\tau_{fl} = 3.38 \times 10^8$ s^{-1}). In addition, the calculated nonradiative rate constant (k_{nr}) of S65T (high pH) is ~1.18×10^8 s^{-1} at 480 nm excitation. Following the Strickler−Berg approach,[32] we also used the absorption and emission spectra of anionic S65T (pH 10) to calculate the radiative rate constant (~2.88×10^8 s^{-1}), which agrees well with the above value.

In an acidic environment (pH < pK_a), the excited anionic-state fluorescence decays as a biexponential (e.g., $\tau_1 = 2.16$ ns, $\alpha_1 = 0.35$, $\tau_2 = 3.05$ ns, and $\alpha_2 = 0.47$ at pH 4.0) with a significantly faster average lifetime of 2.58 ± 0.02 ns. At pH 3.6, the fluorescence decays as a triple exponential ($\tau_1 = 87$ ps, $\alpha_1 = 0.38$, $\tau_2 = 1.29$ ns, $\alpha_2 = 0.34$, $\tau_3 = 3.82$ ns, and $\alpha_3 = 0.28$) with an average lifetime of 1.54 ± 0.06 ns (Table 1, Figure 2D). Under similar conditions, however, FCS studies on anionic S65T revealed fast (up to 350 μs) fluorescence blinking that was attributed to a combination of internal (light-driven) and external (pH-driven) proton transfers.[3,25,37] Since the external proton transfer (from buffer to the protein interior) takes place on a slow time scale (10^{-6}−10^{-4} s), it is unlikely to occur on the potential energy surface of the excited anionic state during the 2.95 ns lifetime.[3,4] Instead, the partitioning of the ground-state population between anionic and neutral S65T can be excited at 488 nm at low pH (Figure 1), albeit with different excitation probabilities due to the Franck−Condon principle. We have measured time-resolved fluorescence polarization anisotropy of S65T, as a function of pH, to examine

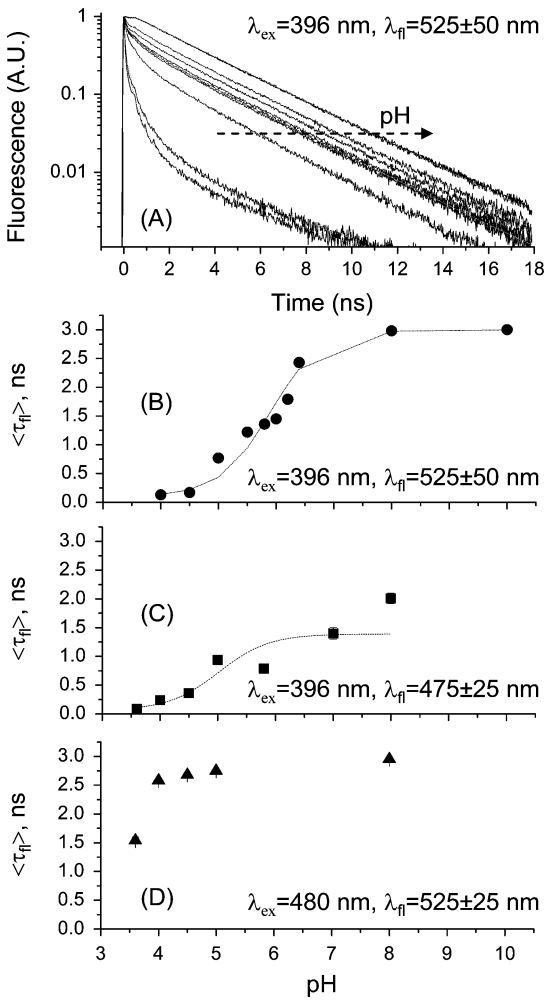

Figure 2. pH sensitivity of the excited-state fluorescence dynamics of S65T dependence on the excitation and detection wavelengths. (A) Representative fluorescence decays of S65T as a function of pH (10.0, 8.0, 6.4, 6.2, 6.0, 5.8, 5.5, 5.0, 4.5, and 4.0), excited at 396 nm with magic angle (54.7°) detection of 525 ± 50 nm emission. (B) Average fluorescence (525 ± 50 nm) average lifetimes are fit with the following equation:[25] $\langle F\rangle\alpha\langle\tau_{fl}\rangle = a + b[1 + 10^{(pK_a - pH)}]^{-1}$, where $a = 0.4 \pm 0.1$, $b = 2.6 \pm 0.1$, and $pK_a = 5.8 \pm 0.1$, which yields $\Delta G° = 33.61$ kJ/mol. (C) Estimated pK_a value is reduced (pK_a = 4.94) when the fluorescence is detected at 475 ± 25 nm. By comparison, the average fluorescence lifetime of anionic S65T exhibits a relatively less pronounced pH dependence (D).

TABLE 2: pH Dependence of the Time-Resolved Fluorescence of Neutral S65T When Excited at 396 nm[a]

pH	τ_1 (ps)	α_1	τ_2 (ns)	α_2	τ_3 (ns)	α_3	$\langle\tau_{fl}\rangle$ (ns)
8.0	100(16)[b]	0.29(1)	1.2(2)	0.32(6)	4.1(3)	0.39(5)	2.01(9)
7.0	90(21)	0.34(2)	0.6(2)	0.28(2)	3.2(4)	0.38(4)	1.4(1)
5.8	85(2)	0.40(2)	0.40(3)	0.32(6)	2.75(3)	0.22(1)	0.79(2)
5.0	84(5)	0.39(1)	0.41(1)	0.34(1)	2.81(2)	0.27(2)	0.94(4)
4.5	77(7)	0.52(2)	0.32(2)	0.40(1)	2.26(3)	0.08(1)	0.36(1)
4.0	60(5)	0.64(1)	0.35(2)	0.31(1)	1.90(5)	0.05(2)	0.24(1)
3.6	36(8)	0.86(1)	0.31(5)	0.13(2)	1.2(2)	0.013(6)	0.09(2)

[a] The fluorescence is detected at 475 ± 25 nm using magic angle (54.7°) polarization with 4.88 ps/channel. [b] The number in parentheses represents the standard deviation (uncertainty) of the last digit.

possible correlation between confirmation changes[43] and fluorescence blinking due to external proton transfer in FCS studies.[25]

3.2.2. pH Effects on the Rotational Diffusion and Structural Conformation of Anionic S65T. The time-resolved fluorescence (525 ± 25 nm) polarization anisotropy of anionic S65T decays as a single exponential with a rotational time $\varphi = 17 \pm 1$ ns and an initial anisotropy of 0.33 ± 0.01, over the range from pH 4.5 to 8.0. The single-exponential anisotropy decay indicates that the embedded anionic chromophore is restricted by the protein environment with an overall hydrodynamic volume of ~78.2 nm^3. In contrast, the fluorescence anisotropy of S65T decays as a biexponential as the pH is reduced below the pK_a value (e.g., $\varphi_1 = 5.1$ ns, $\beta_1 = 0.11$, $\varphi_2 = 28$ ns, and $\beta_2 = 0.22$ at pH 3.6). The observed biexponential anisotropy decay indicates a segmental mobility of the chromophore in a denatured protein at pH 3.6.

These results suggest that the chromophore of anionic S65T is protected by the intact β-barrel, which explains the absence of fluorescence pH blinking in S65T using FCS at high pH.[15,25,26] At very low pH, the ground-state population of neutral S65T increases, with concurrent reduction of the anionic population as well as denaturation of the protein. Consequently, the blinking process in FCS studies of S65T and other GFP mutants, [15,25,26] under similar conditions, is likely due to the conversion of the anionic (i.e., bright) to the neutral (i.e., presumed dark or nonfluorescent) state on the ground-state potential energy surface. However, there are not thorough FCS and conformational studies on the neutral-state transition of GFP mutants as a function of pH. Here, we conducted fluorescence polarization anisotropy and FCS measurements of neutral S65T and EGFP, respectively, as a function of pH.

3.3. Neutral-State Transition Sensitive to pH and Detection Wavelength. *3.3.1. pH Effects on the Neutral-State Fluorescence (475 ± 50 nm).* On the basis of the steady-state spectroscopy (Figure 1) and the energy diagram of the electronic state transitions of S65T (shown below in Figure 6), it is possible to probe the excited neutral-state dynamics of S65T using a combination of excitation (396 nm) and detection (450 ± 25 nm) selectivity. In addition, excited-state proton transfer and/or direct excitation of high vibronic levels may also lead to populating the excited state of anionic GFP mutants. Under 396 nm excitation, the excited-state fluorescence (475 ± 25 nm) of S65T (pH 8.0) decays as a triple exponential with $\tau_1 = 100 \pm 16$ ps, $\alpha_1 = 0.29 \pm 0.01$, $\tau_2 = 1.2 \pm 0.2$ ns, $\alpha_2 = 0.32 \pm 0.06$, $\tau_3 = 4.1 \pm 0.3$ ns, and $\alpha_3 = 0.39 \pm 0.05$ (Table 2). In addition to the multiexponential decay, the estimated average lifetime is 2.01 ± 0.09 ns, as compared to the 2.95 ns measured for the anionic-state transition (Figures 2C and 2D). The fast time constants of the measured triple-exponential decays dominate with pH reduction. At pH 4.0, for example, the fluorescence of neutral S65T decays as a triple exponential with $\tau_1 = 60 \pm 5$ ps, $\alpha_1 = 0.64 \pm 0.01$, $\tau_2 = 0.35 \pm 0.02$ ns, $\alpha_2 = 0.31 \pm 0.01$, $\tau_3 = 1.90 \pm 0.05$ ns, and $\alpha_3 = 0.05 \pm 0.02$ with an average lifetime of 240 ± 10 ps (i.e., $k_{fl}^N = 1/\langle\tau_{fl}^N\rangle \approx 4.17 \times 10^9$ s^{-1}). Figure 2C depicts the average fluorescence lifetime of S65T as a function of pH with an estimated pK_a value of 4.9 ± 0.9. We also used the Strickler−Berg equation[32] with the absorption and emission spectra of neutral S65T (pH 4) to calculate the radiative rate constant ($k_r \approx 6.21 \times 10^8$ s^{-1}). Consequently, the fluorescence quantum yield ($\Phi_{fl}^N = k_r/k_{fl}^N$) of the neutral-state transition in S65T can be roughly estimated ($\Phi_{fl}^N \approx 0.15$), which is significantly lower than the value of 0.65 for the anionic state.[1] As a result, we conclude that the neutral-state transition is relatively nonfluorescent (or dark) due to efficient nonradiative processes that may include proton transfer as well as isomerization pathways. In addition, it is likely that the neutral-state transition is comprised of multiple states ($\langle S^N\rangle$, Figure 6) to account for the observed multiexponential fluorescence decays.

TABLE 3: pH Dependence of the Time-Resolved Fluorescence of S65T When Excited at 396 nm[a]

pH	τ_1 (ps)	α_1	τ_2 (ns)	α_2	τ_3 (ns)	α_3	$\langle\tau_{fl}\rangle$ (ns)
10			2.7(1)[b]	0.43(3)	3.25(5)	0.55(5)	3.00(1)
8.0			2.6(1)	0.54(8)	3.4(1)	0.5(1)	2.98(1)
6.4	403(54)	0.21(5)	2.4(2)	0.3(2)	3.3(2)	0.5(2)	2.43(6)
6.2	102(25)	0.30(1)	0.84(2)	0.17(1)	2.99(3)	0.54(2)	1.79(6)
6.0	98(17)	0.36(1)	0.69(9)	0.21(1)	2.96(1)	0.43(1)	1.45(4)
5.8	94(11)	0.38(1)	0.68(3)	0.23(1)	2.93(2)	0.40(1)	1.36(2)
5.5	87(2)	0.42(4)	0.65(6)	0.26(8)	2.51(1)	0.36(2)	1.22(1)
5.0	88(2)	0.52(4)	0.55(3)	0.28(2)	2.77(1)	0.21(2)	0.77(6)
4.5	48(6)	0.82(3)	0.48(3)	0.16(3)	3.4(2)	0.018(4)	0.169(7)
4.0	45(5)	0.84(8)	0.45(2)	0.12(2)	3.6(5)	0.01(1)	0.13(2)

[a] The total fluorescence (525 ± 50 nm) is detected at magic angle (54.7°) polarization with time/channel of 24.4 ps. [b] The number in parentheses represents the standard deviation (uncertainty) of the last digit.

3.3.2. pH Effects on the Neutral Plus Anionic State Fluorescence (525 ± 50 nm). The partitioning of the ground-state population of anionic, neutral, and intermediate species of GFP is pH-dependent. As a result, it is more informative to assemble most of the ground-state population(s) to examine how the corresponding excited-state dynamics correlates with steady-state thermodynamics. Such collective probing of different S65T populations can be achieved using 396 nm excitation with wide-band emission detection (e.g., 525 ± 50 nm filter). In addition to the direct excitation of the neutral-state transition of S65T, the excited anionic state can also be populated either directly (but with much weaker probability according to the Franck−Condon principle) or indirectly (via excited-state proton transfer or intramolecular energy transfer), as shown in Figures 1 and 6.

When excited at 396 nm, the total fluorescence (525 ± 50 nm) of S65T (pH 10) decays as a biexponential, where $\tau_1 = 2.7 \pm 0.1$ ns, $\alpha_1 = 0.43 \pm 0.03$, $\tau_2 = 3.25 \pm 0.05$ ns, and $\alpha_2 = 0.55 \pm 0.05$ with an estimated average lifetime of 3.00 ± 0.01 ns (Table 3). At low pH (p$K_a = 5.9 \pm 0.1$),[25] the fluorescence decays become triple exponentials with significantly reduced average fluorescence lifetimes (Figures 2A and 2B) as the environment becomes more acidic. At pH 4.0, for example, the fluorescence decay is best described with $\tau_1 = 45 \pm 5$ ps, $\alpha_1 = 0.84 \pm 0.08$, $\tau_2 = 450 \pm 20$ ps, $\alpha_2 = 0.12 \pm 0.02$, $\tau_3 = 3.6 \pm 0.5$ ns, and $\alpha_3 = 0.01 \pm 0.01$ with an average lifetime of 130 ± 20 ps (Table 3). The pH dependence of the average fluorescence lifetime yields a pK_a of 5.8 ± 0.1 (Figure

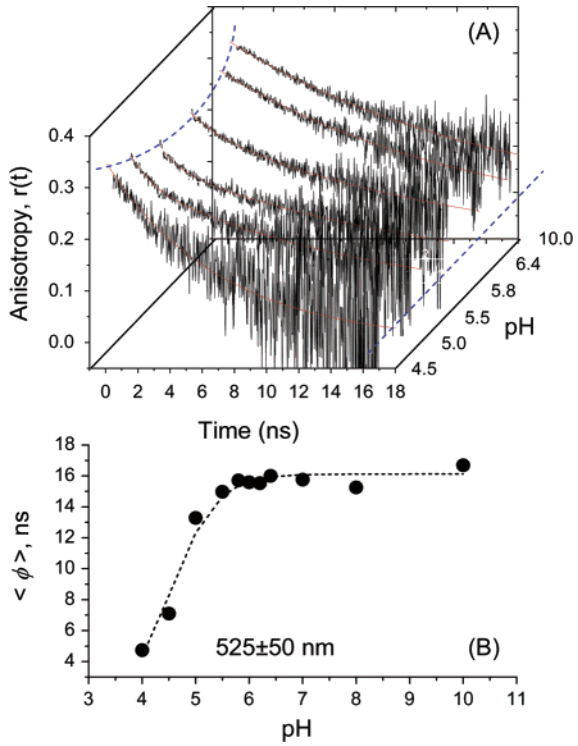

Figure 3. Rotational diffusion and segmental mobility of S65T sensitivity to pH as revealed by time-resolved fluorescence polarization anisotropy. In this experiment, parallel and perpendicular fluorescence polarizations were detected simultaneously, using a wideband filter (bandwidth of 525 ± 50 nm) prior to calculating the anisotropy decays. (A) A single exponential describes the anisotropy decays with ~16 ns rotational time over the pH 6.4−10 range, but a slight reduction of the initial anisotropy can be identified. The observed biexponential at pH 5.8 and 5.5 suggests a segmental mobility of the embodied chromophore in S65T due to partial denaturation (i.e., conformational changes) of the β-barrel. The rotational time of the S65T chromophore becomes faster as the β-barrel denatures in the acidic environment below the pK_a value. The dotted lines serve as a guide through the variation of initial and residual anisotropy with pH. (B) The estimated average rotational time of S65T was calculated from the measured anisotropy decays (shown in Figure 3A) as a function of pH. The estimated pK_a value (4.9 ± 0.2) using these conformational changes of S65T are low compared to the pK_a calculated using the average fluorescence lifetime (Figure 2B).

2B), which is in agreement with literature values obtained by FCS (5.9 ± 0.1),[25] despite the difference between the time scales of slow blinking (greater than or equal to millisecond) and fast excited-state dynamics (picosecond to nanosecond). As a result, we conclude that pH alters the partitioning of the ground-state populations of neutral and anionic states of GFP mutants by modifying the ground-state potential energy surfaces of the anionic and neutral states as well as their barriers.

The results are consistent with the hypothesis that the neutral state(s) of S65T (and possibly other GFP mutants) dominate at a low pH and are relatively dark (i.e., weakly fluorescent) with a lower fluorescence quantum yield ($\Phi_{fl}^{N} \approx 0.15$, see above) than that of the anionic-state transition ($\Phi_{fl}^{A} \approx 0.65$[1]). In an acidic environment, the β-barrel of S65T is partially denatured, altering the net ionic charges by electrostatic repulsion and hydrogen-bond disruption due to excess proton concentration.[38] In addition to the protonation of the chromophore in an acidic environment,[25,39] the observed reduction of fluorescence lifetime (i.e., quantum yield) also suggests that the interruption of the hydrogen-bonding network surrounding the chromophore may lead to cis/trans isomerization,[42,43] as an additional nonradiative mechanism. To examine this hypothesis, we carried out time-resolved fluorescence polarization anisotropy measurements of S65T as a function of pH.

TABLE 4: Time-Fesolved Fluorescence Polarization Anisotropy of GFP−S65T as a Function of pH[a]

pH	ϕ_1 (ns)	β_1	ϕ_2 (ns)	β_2	r_∞	r_0	$\langle\phi\rangle$ (ns)
10			16.7	0.33		0.33	16.7
8.0			15.3	0.33		0.33	15.3
7.0			15.8	0.33		0.33	15.8
6.4			16.1	0.32		0.32	16.1
6.2			15.5	0.31		0.31	15.5
6.0	1.4	0.01	15.8	0.31		0.3[b]	12.0
5.8	1.86	0.03	17.5	0.25		0.28	9.20
5.5	1.1	0.04	17.5	0.23		0.27	5.45
5.0	1.29	0.06	15.9	0.25		0.31	5.00
4.5			7.1	0.35		0.35	7.1
4.0			5.6	0.34	0.06	0.40	5.6
3.6			4.5	0.33	0.04	0.37	4.5

[a] The protein is excited at 396 nm while the total fluorescence emission is detected at 525 ± 50 nm. Similar measurements are also conducted while detecting 475/450 nm as well as the anionic transition (data not shown). [b] The sum of the preexponential terms is the initial anisotropy at zero time.

3.3.3. Segmental Mobility and Conformation Changes of S65T in an Acidic Environment. Figure 3 shows fluorescence polarization anisotropy decays of S65T as a function of pH, and the fitting parameters are summarized in Table 4. Under 396 nm excitation, the time-resolved fluorescence (525 ± 50 nm) anisotropy of S65T (high pH) decays as a single exponential with an estimated rotational time $\varphi = 15.9 \pm 0.3$ ns, which yields a hydrodynamic volume of ~72.6 nm^3, consistent with its molecular weight (29 ± 1 kDa) and X-ray crystal structure.[39] The observed single-exponential decay of polarization anisotropy also implies a rigid S65T protein with an intact β-barrel, which might explain the lack of pH-driven fluorescence blinking in FCS studies at high pH values.[15,25,37]

Near the pK_a (~5.94), the fluorescence polarization anisotropy of S65T decays as a biexponential with $\varphi_1 = 1.4$ ns, $\beta_1 = 0.01$, $\varphi_2 = 15.8$ ns, and $\beta_2 = 0.31$, which indicates a segmental mobility of the chromophore due to a slight denaturation of the protein and, therefore, less restriction inside the β-barrel. The second slow component is the overall rotational time of the protein. As the pH decreases further below the pK_a, the amplitude of the fast decay component increases, suggesting a larger degree of freedom for the segmental mobility (i.e., tumbling) of the chromophore. In addition, the initial anisotropy (r_0) decreases slightly (but consistently) with pH reduction, possibly due to (i) the enhanced rotational mobility of the less-restricted chromophore and/or (ii) intramolecular energy transfer between the excited neutral and anionic states of S65T. Interestingly, further denaturation of the protein at pH ≤ 4.0 leads to a single-exponential anisotropy decay with a rotational time of ~5.6 ns, which is much faster than the rotation of intact S65T protein (e.g., at pH > pK_a). The measured fast rotational time (~5.6 ns), associated with the segmental mobility, of denatured S65T (pH ≤ 4.0) is also too slow to be assigned as a free, fully isolated chromophore. As a result, we conclude that the chromophore is still tethered to the adjacent amino acid backbone via a hydrogen-bond network and remains as an integral part of the denatured protein.

These results suggest that the β-barrel of S65T (and possibly other GFP mutants)[1,2] is denatured in an acidic environment and that the segmental mobility of the embodied chromophore increases with buffer acidity at pH ≤ pK_a. Under these conditions, the chromophore experiences more rotational degrees of freedom (or segmental mobility), even while remaining

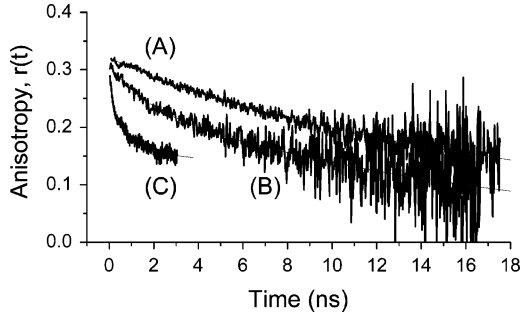

Figure 4. Fluorescence polarization anisotropy of S65T (pH 5.0) reveals wavelength-dependent access to different protein states. The fluorescence anisotropy of S65T (pH5.0) excited at 396 nm decays as a biexponential with $\varphi_1 = 1.7$ ns, $\beta_1 = 0.065$, $\varphi_2 = 17.9$ ns, and $\beta_2 = 0.24$ (B) as compared with a single-exponential decay ($\varphi = 20.3$ ns, $r_0 = 0.32$) of the anionic state under 480 nm excitation (A). Further, the anisotropy associated with 475 ± 50 nm emission is best described as a triple exponential with $\varphi_1 = 100$ ps, $\beta_1 = 0.05$, $\varphi_2 = 763$ ps, $\beta_2 = 0.076$, $\varphi_3 = 24.9$ ns, and $\beta_3 = 0.167$ over a short observation window that is dictated by the corresponding excited-state lifetime (C).

attached to the amino acid backbone of the denatured protein (based on the residual anisotropy observed under acidic environments ($r_\infty \approx 0.06$ at pH 4.0). These real-time ultrafast dynamics indicate that structural changes of S65T in an acidic environment correlate with (i) the external proton transfer from the buffer to the interior moiety of the protein and, therefore, (ii) the loss of GFP fluorescence (i.e., blinking). The observed segmental mobility also suggests an interruption of the hydrogen-bonding network[42,43] between the chromophore and the neighboring amino acid residues upon the denaturation of the protein β-barrel at low pH.[3,4] In the absence of such steric hindrance, therefore, the chromophore becomes less restricted and more likely to undergo cis/trans isomerization, which may explain the observed reduction of (i) initial anisotropy, (ii) the time scale of the segmental mobility, and (iii) fluorescence lifetime as an additional nonradiative pathway, besides proton transfer. This conclusion is also in agreement with molecular dynamics simulations of GFP deprotonation.[29]

Due to the combined influence of pH on the overall rotational diffusion and segmental mobility of the chromophore of S65T, the average rotational time (weighted by the amplitude fractions) can be used to qualitatively assess the pK_a associated with conformational changes as a function of pH. The estimated pK_a value appears dependent on the detection wavelength, where pK_a = 5.2 ± 0.2 and 4.9 ± 0.2 (Figure 3B) using filters with bandwidths of 525 ± 25 nm and 525 ± 50 nm (Figure 3B), respectively. To correlate these ultrafast structural changes of GFP at low pH with fluorescence blinking on the microsecond time scale, we compare them to the FCS results of neutral EGFP at 405 nm excitation, which is almost nonexistent.[30] Furthermore, these measurements will also enable us to examine the role of the neutral-state transition (which is considered dark)[25] in the fluorescence blinking mechanism.

3.3.4. Detection Wavelength Dependence of the Rotational Diffusion of Neutral S65T (pH 5.0). Time-resolved fluorescence polarization anisotropy of S65T (pH 5.0) depends on the detection wavelength (Figure 4). Ultimately, these results may enable us to assign the different electronic state transitions to specific structural conformations of the protein. The fluorescence anisotropy of S65T (pH 5.0), excited at 396 nm, decays as a biexponential, with $\varphi_1 = 1.7$ ns, $\beta_1 = 0.07$, $\varphi_2 = 17.9$ ns, and $\beta_2 = 0.24$ (B), as compared with the single-exponential decay ($\varphi = 20.3$ ns, $r_0 = 0.32$) of the anionic state under 480 nm excitation (A). Further, the anisotropy associated with 475 ± 50 nm emission is best described as a triple exponential with $\varphi_1 = 100$ ps, $\beta_1 = 0.05$, $\varphi_2 = 763$ ps, $\beta_2 = 0.08$, $\varphi_3 = 24.9$ ns, and $\beta_3 = 0.167$ over a short observation window that is dictated by the corresponding excited-state lifetime (C). Due to the bandwidth of the detection filter used here, contributions of different electronic states can be expected. Further, the multiexponential anisotropy decays also indicate a pronounced dependence of the segmental mobility of S65T (pH 5.0) as a function of the detection wavelength.

3.4. Complementary Studies of Fluorescence Blinking of EGFP using FCS. *3.4.1. Fluorescence Blinking of Anionic EGFP.* At pH 11, the correlation curve of anionic EGFP (F64L/S65T), excited at 488 nm, is described mainly by diffusion with $\tau_D = 5.85 \pm 0.09$ ms (i.e., the diffusion coefficient, $D \approx 6.9 \times 10^{-7}$ cm^2/s) and a minor (amplitude fraction, $f_{B1} \approx 0.11$) light-driven blinking time $\tau_{B1} = 450 \pm 50$ μs, in agreement with Haupts et al.[25] The measured diffusion time of EGFP is basically the same at pH 5 under low-intensity excitation. At pH 5, the autocorrelation of anionic EGFP additionally reveals two blinking processes with time constants (amplitude fractions) of 85 μs (0.77) and ~1.1 ms (0.24) that are attributed to external and internal proton transfer processes, respectively.[25] The observed fast blinking component is attributed to external proton exchange between the buffer and the protein interior.[3,25,26,37] Similar measurements have been conducted on other anionic GFP mutants, such as S65T,[25] citrine,[15] pHlurine, and sapphire (H9),[30] and yellow fluorescent proteins (namely, T203Y and T203F)[40] using FCS. The light- and pH-driven conversion between bright and dark states in GFP mutants has been modeled using the ground- and excited-state potential energy surfaces of three electronic transitions including a hypothesized intermediate state.[21,30]

In contrast to the anionic states of EGFP, FCS studies of the neutral states of GFPs are almost nonexistent,[41] even though such studies might address the role of neutral-state transitions in the blinking mechanism of GFPs. Here, we present fluorescence fluctuation dynamics studies of neutral EGFP (excited at 405 nm) using FCS as a function of pH (4.9−11). These measurements enable us to correlate the fast structural changes of GFP reported above with the slow blinking dynamics of the neutral and anionic states.

3.4.2. Fluorescence Blinking of the Excited Neutral-State Transition of EGFP. The overall autocorrelation function can be described adequately using the product of the diffusion and blinking functions (eqs 4 and 5): $G(\tau) = G_D(\tau) \cdot G_B(\tau)$.[25] The autocorrelation curve of neutral EGFP (pH 11) is best described by diffusion ($\tau_D = 1.78 \pm 0.08$ ms) with a blinking component ($\tau_{B1} = 7 \pm 3$ μs, $f_{B1} \approx 0.48$) that is significantly faster than the anionic EGFP light-driven blinking ($\tau_{B1} = 450 \pm 50$ μs, $f_{B1} \approx 0.11$). The calculated diffusion coefficient of neutral EGFP (pH 11) is ~2.2×10^{-7} cm^2/s, which is slightly smaller than that of anionic EGFP diffusion (~6.9×10^{-7} cm^2/s) and likely due to different photophysics of both EGFP and the reference (rhodamine green) under 396 and 488 nm excitation. The fast blinking component, which seems pH-independent (Figure 5A), is tentatively attributed to light-driven blinking between the bright and the dark states of the protein.[3,25,26,37] The significance of this fast decay component is likely to be compromised by the low signal-to-noise (Figure 5A) and the so-called "after pulsing" inherent in the avalanche photodiodes.[16] As the acidity of the buffer is increased (pH ≤ pK_a), the fractional amplitude of an additional blinking component (f_{B2}) increases, and the pH-dependent time constant (τ_{B2}) decreases with an estimated pK_a of 5.77 ± 0.08 (Figure 5B). The observed differences of the

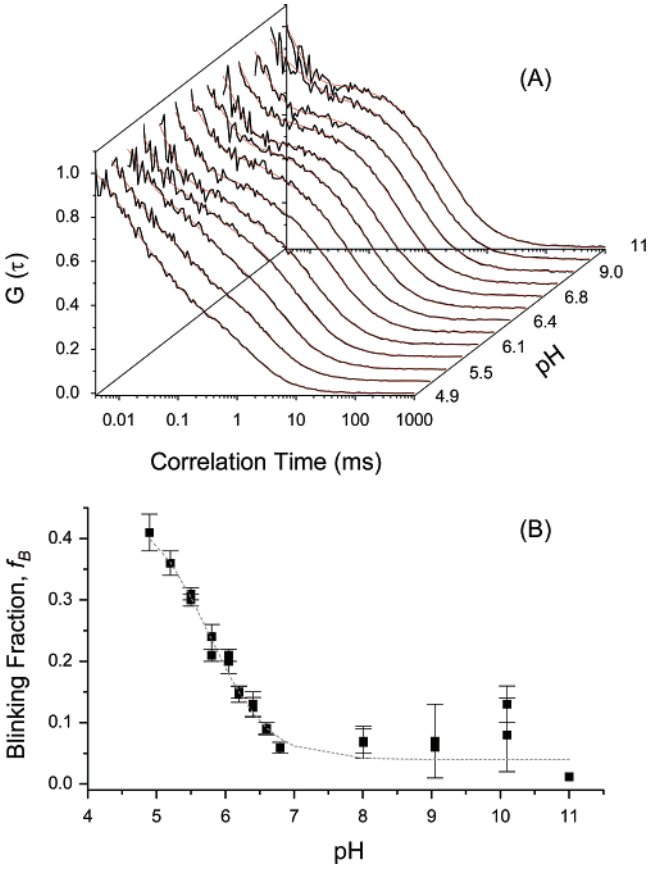

Figure 5. Complementary FCS studies of neutral EGFP (F64L/S65T), which was excited at 405 nm, as a function of pH. Haupts et al. have demonstrated that the pH dependence of EGFP and GFP−S65T mutants exhibits comparable photoconversion kinetics under 488 nm excitation (i.e., the anionic-state transition).[25] The autocorrelation curves (A) of neutral EGFP are best described by diffusion and blinking terms (see eq 5). The amplitude fraction of the blinking population of EGFP, as a function of pH, yields p$K_a \approx 5.76$ (B), which is slightly smaller than that of the anionic-state transition (p$K_a \approx 5.9$) of EGFP.[25]

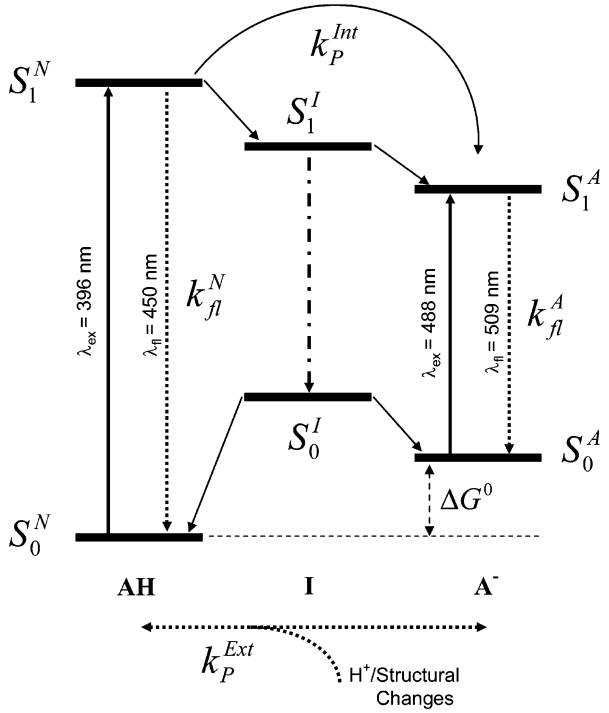

Figure 6. Schematic energy diagram of the neutral (AH), anionic (A^-), and hypothesized intermediate (I) electronic state transitions of GFP−S65T (and possibly other GFP mutants). The electronic energy between the corresponding ground (S_0^N,S_0^A) and first excited (S_1^N,S_1^A) states for each transition can be calculated using steady-state spectroscopy (Figure 1), except the intermediate state transition ($S_0^I \rightarrow S_1^I$). The proposed scheme also accounts for excited-state relaxation dynamics (e.g., neutral k_{fl}^N and anionic k_{fl}^A fluorescence decay rates) as well as photoconversion via either external (k_P^{Ext}, pH-driven) or internal (k_P^{Int}, light-driven) proton transfer, which are observed using time-resolved fluorescence and FCS measurements as a function of pH and excitation/detection wavelength. The observed reduction of the excited-state fluorescence lifetime and segmental mobility of the GFP chromophore, at low pH, indicates a correlation between ultrafast conformational changes of the protein structure and external proton transfer (from low-pH buffer to the protein interior) in acidic environments.

time constants and the amplitude fractions between neutral and anionic EGFP can be attributed to the nature of the potential energy surfaces and barrier heights of the corresponding electronic state transitions.[21,15,30]

3.5. Modeling the Electronic Transitions and Photoconversion in GFP−S65T. On the basis of our studies of both fast excited-state dynamics[3] (using time-resolved fluorescence and polarization anisotropy) and slow fluorescence blinking processes[25] (using FCS) of GFP−S65T and EGFP, we propose an energy diagram[3,4] of different state transitions (Figure 6) and the following conclusions emerge. First, the β-barrel of anionic GFP (at high pH and 488 nm excitation) is intact and exerting a constraining force on the embedded chromophore leading to negligible nonradiative pathways such as cis/trans isomerization and external proton exchange with the buffer. Second, the excited neutral state of S65T can be excited at 396 nm and detected selectively around 450 ± 25 nm. In addition, the anionic-state transition of GFP can be excited at 396 nm via either direct excitation (but with a low Franck−Condon factor) or excited-state internal proton transfer (k_P^{Int}), as observed in some GFP mutants. Third, our FCS studies of the neutral EGFP, for the first time, suggest that the neutral-state transition is involved with GFP fluorescence blinking. The observed kinetics also confirm the hypothetical intermediate state as the dark state invoked in previous studies in GFP fluorescence. Fourth, the time scales associated with the excited-state dynamics (picosecond to nanosecond) and fluorescence blinking (microsecond to millisecond) are distinctly different, which indicates that the observed pH-driven conversion is likely to occur on the ground-state potential energy surface. Despite these differences, the estimated pK_a values using ultrafast time-resolved fluorescence agree well with the FCS results. As a result, the observed multiexponential fluorescence decays of neutral GFP (low pH) are assigned to the excitation of multiple, ground-state GFP conformations (or states) that exist at equilibrium. Fifth, the observed conformational changes of the β-barrel and the amino acids surrounding the chromophore are likely to facilitate external proton transfer from the buffer to the protein interior, which underlies the fluorescence blinking of GFPs. In an acidic environment, these conformational changes of the β-barrel and the disruption of the hydrogen-bonding network reduce the restriction on the GFP chromophore and, therefore, may lead to an isomerization pathway.[42,43] With the experimental results provided here, however, it is difficult to be more specific concerning the isomerization mechanism involved (e.g., whether it involves Thr203)[42,43] or the exact configuration (trans, cis, or hula twist)[44] associated with neutral and anionic states of these GFP mutants. While these conclusions may be generalized to other GFP mutants, the rates and amplitude fractions associated with blinking and conformational changes are likely to depend on pH and mutation site/type.[15] We are currently

applying the same experimental approach to determine whether these findings are still valid in the new generation of monomeric red fluorescent proteins that have been engineered recently by Tsien and co-workers.[16]

4. Conclusion

Time-resolved fluorescence and polarization anisotropy measurements of GFP−S65T are carried out as a function of pH (3.6−10.0) as well as excitation and detection wavelengths. At high pH, the β-barrel of anionic GFP−S65T is intact with a rotational time consistent with its molecular weight, which explains the absence of pH-dependent fluorescence blinking in FCS studies. As the pH reduced below the pK_a value (∼5.9), the average fluorescence lifetime decreases (by ∼18%) with minor conformational changes (except at pH 3.6). The pH effects on the total S65T fluorescence dynamics and conformational changes become more pronounced upon assembling different ground-state populations under 396 nm excitation. The observed segmental mobility in an acidic environment indicates that the embodied chromophore becomes less restricted by the surrounding hydrogen-bonding network and the amino acids. Such conformational changes of the protein coincide with pH-driven fluorescence blinking due to external proton transfer using fluorescence correlation spectroscopy, which occurs on much slower time scales. As a result, we conclude that structural changes of the β-barrel at low pH facilitate external proton transfer from the low-pH buffer to the protein moiety. Furthermore, the observed changes in S65T structure may also trigger cis/trans isomerization of the chromophore as an additional nonradiative pathway. Due to these conformational changes and fluorescence sensitivity as a function of pH, GFP mutants can be used as efficient noninvasive pH sensors for biological studies.

Acknowledgment. We thank Professor Stephen Benkovic (Department of Chemistry, Penn State University) for the gift of purified GFP-S65T. The FCS measurements on EGFP were carried out in the laboratory of Professor Watt Webb (Developmental Resource for Biophysical Imaging Opto-Electronics Laboratory, Cornell University). We are also thankful for the comments and critiques of Angel Davey and Dr. Michael E. Webb (Department of Chemistry, Penn State University). This work was supported by the Penn State Materials Research Institute and the Penn State Materials Research Science and Engineering Center (supported by the National Science Foundation (NSF), Grant No. DMR 0213623) and the Lehigh−Penn State Center for Optical Technologies (supported by the Commonwealth of Pennsylvania). Additional support was also provided by the Huck Institutes of the Life Sciences (Penn State University). The help of Chieh-Hsin Kuan, at the early stage of this project, is deeply appreciated. H.-R. K. also acknowledges the support of the Biomaterial and Bionanotechnology Summer Institute (a National Institutes of Health and NSF undergraduate program; Department of Bioengineering, Penn State University). Finally, we are also grateful to Coherent Lasers, Inc., for their generous loan of a pulse picker (MIRA9200, Coherent).

References and Notes

(1) Tsien, R. Y. *Annu. Rev. Biochem.* **1998**, *67*, 509−544.
(2) *Green Fluorescent Protein: Properties, Applications, and Protocols*, 2nd ed.; Chalfie, M., Kain, S. R., Eds.; Methods of Biochemical Analysis 47; Wiley-Intersciences: Hoboken, NJ, 2005.
(3) Heikal, A. A.; Hess, S. T.; Webb, W. W. *Chem. Phys.* **2001**, *274*, 37−55.
(4) Cody, C. W.; Prasher, D. C.; Westler, W. M.; Prendergast, F. G.; Ward, W. W. *Biochemistry* **1993**, *32*, 1212.
(5) Zimmer, M. *Chem. Rev.* **2002**, *102*, 759−781.
(6) Chalfie, M.; Tu, Y.; Euskirchen, G.; Ward, W.; Prasher, D. C. *Science* **1994**, *263*, 802.
(7) Quillin, M. L.; Anstrom, D. M.; Shu, X.; O'Leary, S.; Kallio, K.; Chudakov, D. M.; Remington, S. J. *Biochemistry* **2005**, *44*, 5774−5787.
(8) Andresen, M.; Wahl, M. C.; Stiel, A. C.; Grater, F.; Schafer, L. V.; Trowitzsch, S.; Weber, G.; Eggeling, C.; Grubmuller, H.; Hell, S. W.; Jakobs, S. *Proc. Natl. Acad. Sci. U.S.A.* **2005**, *102*, 13070−13074.
(9) Zhang, J.; Campbell, R. E.; Ting, A. Y.; Tsien, R. Y. *Nat. Rev. Mol. Cell Biol.* **2002**, *3*, 906−918.
(10) Tsien, R. Y. *FEBS Lett.* **2005**, *579*, 927−932.
(11) Griesbeck, O.; Baird, G. S.; Campbell, R. E.; Zacharias, D. A.; Tsien, R. Y. *J. Biol. Chem.* **2001**, *276*, 29188−29194.
(12) Baird, G. S.; Zacharias, D. A.; Tsien, R. Y. *Proc. Natl. Acad. Sci. U.S.A.* **2000**, *97*, 11984−11989.
(13) Matz, M. V.; Fradkov, A. F.; Labas, Y. A.; Savitsky, A. P.; Zaraisky, A. G.; Markelov, M. L.; Lukyanov, S. A. *Nat. Biotechnol.* **1999**, *17*, 969−973.
(14) Tsien, R. Y. *Nat. Biotechnol.* **1999**, *17*, 956−957.
(15) Heikal, A. A.; Hess, S. T.; Baird, G. S.; Tsien, R. Y.; Webb, W. W. *Proc. Natl. Acad. Sci. U.S.A.* **2000**, *97*, 11996−12001.
(16) Shaner, N. C.; Campbell, R. E.; Steinbach, P. A.; Giepmans, B. N. G.; Palmer, A. E.; Tsien, R. Y. *Nat. Biotechnol.* **2004**, *22*, 1567−1572.
(17) Elowitz, M. B.; Surette, M. G.; Wolf, P. E.; Stock, J.; Leibler, S. *Curr. Biol.* **1997**, *7*, 809−812.
(18) Stepanenko, O. V.; Verkhusha, V. V.; Kazakov, V. I.; Shavlovsky, M. M.; Kuznetsova, I. M.; Uversky, V. N.; Turoverov, K. K. *Biochemstry* **2004**, *43*, 14913−14923.
(19) Heim, R.; Prasher, D. C.; Tsien, R. Y. *Proc. Natl. Acad. Sci. U.S.A.* **1994**, *91*, 12501−12504.
(20) Heim, R.; Cubitt, A. B.; Tsien, R. Y. *Nature* **1995**, *373*, 663−664.
(21) Dickson, R. M.; Cubitt, A. B.; Tsien, R. Y.; Moerner, W. E. *Nature* **1997**, *388*, 355−358.
(22) Chattoraj, M.; Kong, B. A.; Bublitz, G. U.; Boxer, S. G. *Proc. Natl. Acad. Sci. U.S.A.* **1996**, *93*, 8362−8367.
(23) Lossau, H.; Kummer, A.; Heinecke, R.; Pöllinger-Dammer, F.; Kompa, C.; Bieser, G.; Jonsson, T.; Silva, C. M.; Yang, M. M.; Youvan, D. C.; Michel-Beyerle, M. E. *Chem. Phys.* **1996**, *213*, 1−16.
(24) Volkmer, A.; Subramaniam, V.; Birch, D. J. S.; Jovin, T. M. *Biophys. J.* **2000**, *78*, 1589−1598.
(25) Haupts, U.; Maiti, S.; Schwille, P.; Webb, W. W. *Proc. Natl. Acad. Sci. U.S.A.* **1998**, *95*, 13573−13578.
(26) Hess, S. T.; Huang, S.; Heikal, A. A.; Webb, W. W. *Biochemistry* **2002**, *41*, 697−705.
(27) Baldini, G.; Cannone, F.; Chirico, G. *Science* **2005**, *309*, 1096−1100.
(28) Enoki, S.; Saeki, K.; Maki, K.; Kuwajima, K. *Biochemstry* **2004**, *43*, 14238−14248.
(29) Patnaik, S. S.; Trohalaki, S.; Pachter, R. *Biopolymers* **2004**, *75*, 441−452.
(30) Hess, S. T.; Heikal, A. A.; Webb, W. W. *J. Phys. Chem. B* **2004**, *108*, 10138−10148.
(31) Axelrod, D. *Methods Cell Biol.* **1989**, *30*, 333−352.
(32) Lakowicz, J. R. *Principles of Fluorescence Spectroscopy*, 2nd ed.; Kluwer Academic: New York, 1999.
(33) Patterson, G. H.; Knobel, S. M.; Sharif, W. D.; Kain, S. R.; Piston, D. W. *Biophys. J.* **1997**, *73*, 2782−2790.
(34) Ward, W. W.; Bokman, S. H. *Biochemistry* **1982**, *21*, 4535−4540.
(35) Llopis, J.; McCaffery, J. M.; Miyawaki, A.; Farquhar, M. G.; Tsien, R. Y. *Proc. Natl. Acad. Sci. U.S.A.* **1998**, *95*, 6803.
(36) Miesenbock, G.; DeAngelis, D. A.; Rothman, J. E. *Nature* **1998**, *394*, 192−195.
(37) Schwille, P.; Kummer, S.; Heikal, A. A.; Moerner, W. E.; Webb, W. W. *Proc. Natl. Acad. Sci. U.S.A.* **2000**, *97*, 151−156.
(38) Nelson, D. L.; Cox, M. M. *Lehninger Principles of Biochemistry*, 3rd ed.; Worth Publishers: New York, 2000.
(39) Brejc, J.; Sixma, T.; Kitts, P. A.; Kain, S. R.; Tsien, R. Y.; Ormö, M.; Remington, J. S. *Proc. Natl. Acad. Sci. U.S.A.* **1997**, *94*, 2306−2311.
(40) Schwille, P.; Kummer, S.; Heikal, A. A.; Moerner, W. E.; Webb, W. W. *Proc. Natl. Acad. Sci. U.S.A.* **2000**, *97*, 151−156.
(41) Heikal, A. A.; Webb, W. W. *Proc. SPIE−Int. Soc. Opt. Eng.* **2002**, *4812*, 1−14.
(42) Warren, A.; Zimmer, M. *J. Mol. Graphics Modell.* **2001**, *19*, 297−303.
(43) Elsliger, M. A.; Wachter, R. M.; Hanson, G. T.; Kallio, K.; Remington, S. J. *Biochemistry* **1999**, *38*, 5296−5301.
(44) Weber, W.; Helms, V.; McCammon, J. A.; Langhoff, P. W. *Proc. Natl. Acad. Sci. U.S.A.* **1999**, *96*, 6177−6182.